

A Role for Nrf2 Expression in Defining the Aging of Hippocampal Neural Stem Cells

Cell Transplantation
2018, Vol. 27(4) 589–606
© The Author(s) 2018
Reprints and permission:
sagepub.com/journalsPermissions.nav
DOI: 10.1177/0963689718774030
journals.sagepub.com/home/cll


S. Ray^{1,2,3}, M. J. Corenblum¹, A. Anandhan¹, A. Reed^{1,3},
F. O. Ortiz^{1,3}, D. D. Zhang⁴, C. A. Barnes^{5,6}, and L. Madhavan^{1,6}

Abstract

Redox mechanisms are emerging as essential to stem cell function given their capacity to influence a number of important signaling pathways governing stem cell survival and regenerative activity. In this context, our recent work identified the reduced expression of nuclear factor (erythroid-derived 2)-like 2, or Nrf2, in mediating the decline in subventricular zone neural stem progenitor cell (NSPC) regeneration during aging. Since Nrf2 is a major transcription factor at the heart of cellular redox regulation and homeostasis, the current study investigates the role that it may play in the aging of NSPCs that reside within the other major mammalian germinal niche located in the subgranular zone (SGZ) of the dentate gyrus (DG) of the hippocampus. Using rats from multiple aging stages ranging from newborn to old age, and aging Nrf2 knockout mice, we first determined that, in contrast with subventricular zone (SVZ) NSPCs, Nrf2 expression does not significantly affect overall DG NSPC viability with age. However, DG NSPCs resembled SVZ stem cells, in that Nrf2 expression controlled their proliferation and the balance of neuronal versus glial differentiation particularly in relation to a specific critical period during middle age. Also, importantly, this Nrf2-based control of NSPC regeneration was found to impact functional neurogenesis-related hippocampal behaviors, particularly in the Morris water maze and in pattern separation tasks. Furthermore, the enrichment of the hippocampal environment via the transplantation of Nrf2-overexpressing NSPCs was able to mitigate the age-related decline in DG stem cell regeneration during the critical middle-age period, and significantly improved pattern separation abilities. In summary, these results emphasize the importance of Nrf2 in DG NSPC regeneration, and support Nrf2 upregulation as a potential approach to advantageously modulate DG NSPC activity with age.

Keywords

Nrf2, neural stem cells, aging, dentate gyrus, redox, transplantation

Introduction

Active stem cells possess the capacity to generate new nerve cells, and exist as sources of plasticity throughout life in all vertebrate species^{1,2}. However, with advancing age, these stem cells undergo a significant regenerative decline^{3–5}. The precise mechanisms underlying this core aging process are not fully understood. In this context, we recently reported the reduced expression of the redox-sensitive transcription factor, Nrf2, as an important molecular mediator of subventricular zone (SVZ) neural stem progenitor cell (NSPC) regeneration with age⁶. In particular, these studies identified a critical time-period during middle age, when a marked reduction in SVZ NSPC survival and regenerative capacity occurs, and determined that decreased Nrf2 expression played an important role in mediating this phenomenon.

- ¹ Department of Neurology, University of Arizona, Tucson, AZ, USA
- ² Undergraduate Biology Research Program, University of Arizona, Tucson, AZ, USA
- ³ Neuroscience and Cognitive Science Undergraduate Program, Tucson, AZ, USA
- ⁴ Pharmacology and Toxicology, University of Arizona, Tucson, AZ, USA
- ⁵ Departments of Psychology & Neuroscience, University of Arizona, Tucson, AZ, USA
- ⁶ Evelyn F. McKnight Brain Institute, University of Arizona, Tucson, AZ, USA

Submitted: November 10, 2017. Revised: March 3, 2018. Accepted: March 30, 2018.

Corresponding Author:

L. Madhavan, Department of Neurology, University of Arizona, 1501, N Campbell Ave, Tucson, AZ 85724, USA.
Email: lmadhavan@email.arizona.edu



Creative Commons Non Commercial CC BY-NC: This article is distributed under the terms of the Creative Commons Attribution-NonCommercial 4.0 License (<http://www.creativecommons.org/licenses/by-nc/4.0/>) which permits non-commercial use, reproduction and distribution of the work without further permission provided the original work is attributed as specified on the SAGE and Open Access pages (<https://us.sagepub.com/en-us/nam/open-access-at-sage>).

Nrf2 is a master transcription factor known to be a key regulator of cellular stress⁷⁻⁹. In fact, Nrf2 is essential to the cell's homeostatic mechanism, especially through its capacity to stimulate the expression of multiple cell survival mechanisms in response to oxidative stress and other insults^{8,10}. More than 200 genes that contain antioxidant response elements in their regulatory region are known to be activated by Nrf2. Moreover, Nrf2 can also stimulate numerous other pathways and contribute to a diverse set of cellular functions including energy and nutrient metabolism, autophagy, proteasomal degradation, DNA repair, mitochondrial physiology, cell growth, self-renewal, differentiation, proliferation, and increased lifespan¹¹⁻¹⁶. In this regard, our recent work has added another important new face to Nrf2 actions in the cell, namely the regulation of SVZ NSPC function during aging⁶. These findings have wide ranging relevance towards understanding fundamental aspects of NSPC biology, spanning across other NSPC domains.

From this perspective, the current study investigates the role of Nrf2 in NSPCs existing within the other major neurogenic niche, the subgranular zone (SGZ) of the dentate gyrus (DG) of the hippocampus, which also experiences a regenerative compromise with age^{4,17}. The age-related decay in hippocampal regeneration is important to understand given the relevance of DG neurogenesis to higher cognitive functions, especially memory processes, and particular affective behaviors¹⁸. A recent report has examined Nrf2's influence on DG NSPCs; however, Nrf2's involvement in DG NSPC function during normal aging has not been previously assessed¹⁹. Here, here we conduct a detailed analysis of Nrf2 expression and effects in DG NSPCs utilizing several groups of rats across the lifespan, as well as aging Nrf2 WT and knockout mice. Additionally, we also examine whether the supplementation of the aged hippocampus with ex vivo grown NSPCs, transduced to express high levels of Nrf2, can improve aging DG NSPC function.

Materials and Methods

Animals

Adult male Fisher 344 rats aged 2 mo (young adult or YA), 9 mo (adult or A), 15 mo (middle-aged or MA), and 24 mo of age (old or O), along with newborn (N) postnatal day 0 pups were used (NIH-NIA, Bethesda, MD; Harlan Laboratories, Indianapolis, IN, USA). Corresponding ages in human years are mentioned in the table in Fig 1A. Additionally, 11 and 13 mo old rats were also used in some experiments. Newborn (postnatal day 0) and young adult (2.5 mo) WT (Nrf2^{+/+}) and knockout (Nrf2^{-/-}) C57BL/6 mice were obtained from a colony maintained by Dr Donna Zhang's laboratory (the University of Arizona, AZ, USA). All animals were housed at The University of Arizona Animal Care Facility, and were kept on a reverse 12-hour light-dark cycle with food and water available ad libitum. The animals were treated according to the rules and regulations of the National Institutes of Health and Institutional Guidelines on the Care and Use of Animals,

and The University of Arizona Institutional Animal Care and Use Committee approved all experimental procedures.

In order to isolate primary NSPCs, animals were sacrificed using sodium pentobarbital (60 mg/kg), after which hippocampal tissue was microdissected and processed. For histology, animals were perfused with 4% paraformaldehyde (PFA; Electron Microscopy Sciences, Hatfield, PA, USA), after which brains were extracted and sectioned in the coronal plane at 35 μ m on a freezing sliding microtome or on a cryostat at 10 μ m thickness.

Transplantation Experiments

For the transplantation experiments, newborn or middle-aged NSPCs isolated from the SVZ were transduced with recombinant adeno-associated viral vectors (AAV2/1) encoding Nrf2 (pAAV-CMV-Nfe2l2-IRES-eGFP) or enhanced green fluorescent protein (eGFP) (pAAV-CMV-eGFP) as a control. The viruses had been generated at the Children's Hospital of Philadelphia Viral Vector Core, PA, USA (https://ccmt.research.chop.edu/cores_rvc.php). The viral treatment occurred at a dose of 1×10^5 vg/cell for 6 h.

After about 10 days in culture, the NSPCs (in 2 μ Ls of Hank's balanced salt solution (HBSS; Life Technologies, Grand Island, NY, USA) at 50,000 cells/ μ L) were implanted bilaterally, into two sites along the rostrocaudal axis of the hippocampus (anterior-posterior (AP) -3.0, medial-lateral (ML) \pm 2.8, dorsal-ventral (DV) -4; Site 2: AP -4.08, ML \pm 2.2, DV -2.5), via stereotaxic methods described previously^{20,21}. Animals injected with only HBSS were also included as controls. The number of animals in each experimental group were as follows: Control (HBSS, $n = 5$); N-NSPCs rAAV2/1-eGFP ($n = 7$); N-NSPCs rAAV2/1-Nrf2-eGFP ($n = 6$); MA-NSPCs rAAV2/1-eGFP ($n = 5$); MA-NSPCs rAAV2/1-Nrf2-eGFP ($n = 5$).

Intraperitoneal (i.p.) bromodeoxyuridine (BrdU) injections at a dose of 50 mg/kg/12 h for 3 days before transplantation were administered to all animals. Our previous studies have shown that the administration of BrdU before transplantation labels dividing NSPCs in the SVZ and DG germinal niches of the naïve brain, allowing us to track the response of these endogenous precursors to NSPC transplantation^{20,22}. Additionally, a single injection of 5-ethynyl-2'-deoxyuridine (EdU) was administered ip at 50 mg/kg, 2 mo after transplantation, to examine proliferative activity of grafted NSPCs²³.

NSPC transplanted and control animals were sacrificed using pentobarbital (60 mg/kg), perfused with 4% paraformaldehyde (PFA), extracted brains post-fixed in 4% PFA solution, sunk through a 30% sucrose solution, and sectioned in the coronal plane (35 μ m) on a freezing sliding microtome for morphological studies.

Behavioral Analysis

Morris Water Maze. Spatial learning and memory was determined using the Morris water maze task which involves a

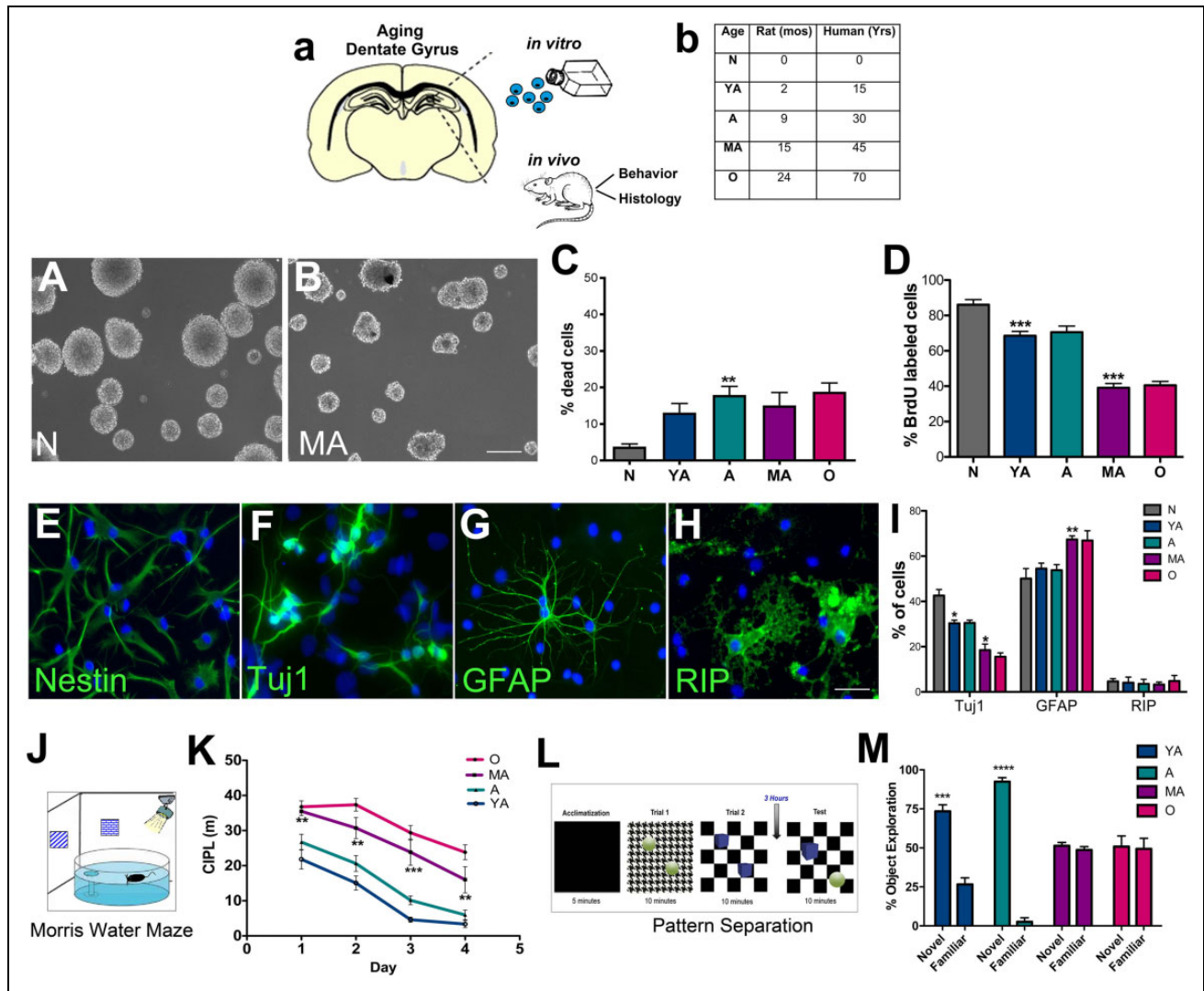


Fig. 1. In vitro characterization and related behavioral analysis of hippocampal NSPC survival and regenerative function across age. The schematic in (A) depicts the experimental design. The main age-groups of rats (with corresponding human years) used in the study are shown in (B). NSPCs were cultured from these rats in vitro studies, and the animals were also behaviorally and histologically assessed. A–B are representative phase-contrast images of newborn and middle-aged NSPCs grown as neurospheres in culture. In vitro analysis of viability and proliferation via live-dead and BrdU assays are shown in C and D (C; $p < 0.01$, YA versus A; D; $p < 0.001$, YA versus A and A versus MA; One-way ANOVA with Tukey's post-hoc test). E–H show examples of undifferentiated NSPCs (E, nestin⁺) and NSPCs which differentiated into Tuj1⁺ neurons (F), GFAP⁺ astrocytes (G) and RIP⁺ oligodendrocytes (H). The graph in I shows quantification of this capacity across the five age-groups in (Tuj1⁺ - $p < 0.05$, N versus YA; $p < 0.05$, A versus MA, one-way ANOVA with Tukey's post-hoc test; GFAP⁺ - $p < 0.01$, A versus MA, one-way ANOVA with Tukey's post-hoc test). The diagram in J shows the Morris water maze behavior analysis set-up and K depicts the results of the task conducted on the different age-groups of rats (K; A versus MA, Two-way RM-ANOVA with Tukey's post-hoc test). Similarly, the experimental set-up of the pattern separation task is shown in L, and results are in M (YA $p < 0.001$ and A $p < 0.0001$, unpaired *t* tests). * $p < 0.05$, ** $p < 0.01$, *** $p < 0.001$. Scale Bars: A: 50 μ m, B: 200 μ m, E–H: 20 μ m. A: adult; ANOVA: analysis of variance; BrdU: bromodeoxyuridine; GFAP: glial fibrillary acidic protein; MA: middle-aged; NSPC: neural stem progenitor cell; YA: young adult.

rodent swimming until it finds a hidden escape platform in a pool of water using the distal visual cues in the room^{24,25}. Briefly, animals were tested in a circular tank (183 cm in diameter) of opaque water containing a submerged platform and fixed visual cues around the room. The animals were assessed over a period of 6 days. The first 4 days

encompassed a spatial task where the animals located the hidden escape platform, and the last 2 days involved a visual task where the platform was raised above the water line. A total of six trials per day were completed, with a rest period between every block of two trials, which were recorded with a video camera placed above the center of the

tank. ANY-maze software (Stoelting Co., Wood Dale, IL, USA) was used to run trials and calculate the corrected integrated path length (CIPL), which corrects for swim speed and release location.

Reversal Task. A modified version of the Morris water maze task with an additional reversal learning component (on days 5 and 6) was utilized for mice. Reversal learning in the Morris water maze demonstrates an animal's ability to learn a new target goal position in the same general spatial context as the initial platform location²⁵. First, at the end of day 4 of the water maze, a probe trial where the hidden platform is removed was conducted. Focal searching behavior in the probe trials was assessed through quantification of the number of goal (just previous location of platform) crossings²⁶. Then the reversal task was initiated and continued over days 5 and 6. This part included six trials per day divided into blocks of two trials during which the hidden platform was moved 180 degrees in the opposite direction from its original location.

Pattern Separation. The pattern separation task examines the animal's ability to distinguish between highly similar events and was performed following protocols from Jain and colleagues (2012) with some modifications^{27–29}. Briefly, rats and mice were habituated to the testing room prior to training. During the training period, animals were placed in an open chamber (30 cm × 30 cm with 30 cm high walls) with a specific floor pattern and two identical objects, and were allowed to explore for 10 min. Following a 30-min inter-trial interval, animals were placed in the box now containing a different floor pattern and two identical objects unique from the objects in the first trial. After 3 h of rest, the testing period was started during which the animals were placed in the box for 10 min with the floor pattern from either trial one or trial two, one object from trial one, and one object from trial two. Time spent exploring the novel object (i.e. the object from trial one in the context from trial two) was compared with the time spent exploring the familiar object (i.e. the object from trial two in the context from trial two). The exploration time of each object was scored manually by the experimenter from captured videos and was defined as the length of time the animal spent actively interacting with the object (when the mouse's nose was 1 cm away from the object).

NSPC Culture

DG NSPCs were isolated from the hippocampi of newborn rats, the different adult rat age-groups, and *Nrf2*^{-/-} and WT mice. All cells were grown under standard conditions, at 37°C and 5% CO₂ following previously established protocols⁶. Newborn cells were cultured in Neurobasal-A Medium containing 1% GlutaMAX[™], 2% B-27, 1% Antibiotic-Antimycotic (Life Technologies, Grand Island, NY, USA), 20 ng/ml epidermal growth factor (EGF), 10 ng/ml basic fibroblast growth factor (bFGF; Cell Sciences, Canton,

MA, USA), and 2 µg/ml of heparin (Stemcell Technologies, Vancouver, BC, Canada). Half the media was replenished every 3 days and cells were passaged every 4–5 days. Adult NSPCs were maintained in Neurobasal-A Medium containing 1% GlutaMAX[™], 2% B-27, 1% Antibiotic-Antimycotic, 20 ng/ml EGF, 20 ng/ml bFGF, and 2 µg/ml of heparin. 50% of media was replenished every 3 days, and the cells were passaged every 7–10 days. All experiments were conducted consistently on passage 1–4 NSPCs, with every assay using at least *n* = 3 independent NSPC cultures, grown in parallel, and examined in triplicate for each age group.

NSPC Viability

A live-dead cell assay kit (Life Technologies) was used to assess NSPC viability, according to previously established protocols⁶. Briefly, cells were plated on poly-D-lysine/laminin (Sigma-Aldrich, St. Louis, MO, USA)-coated glass coverslips (Sigma-Aldrich), and placed in 24 well plates with growth medium. Media was subsequently removed and the cells exposed to 4 µM ethidium homodimer 1 and 2 µM calcein AM dye in 1× phosphate buffered saline (PBS; Life Technologies). After 45 min, the number of green cells (live, labeled with calcein AM dye) and red cells (dead, labeled with ethidium homodimer 1) were counted in five random fields per coverslip under a 20× lens. At minimum, *n* = 3 independent NSPC cultures, grown in parallel, were assessed in triplicate for each age group of cells examined.

NSPC Proliferation

A Bromodeoxyuridine (BrdU) assay was applied to assess proliferation according to previous protocols⁶. NSPCs were plated on poly-D-lysine/laminin-coated glass coverslips, and treated with 10 µM BrdU (Sigma-Aldrich) for 1.5 h. Cells were then washed with 1× PBS (Life Technologies) and fixed using 4% PFA (Electron Microscopy Sciences). The fixed NSPCs were immunostained with antibodies targeting BrdU, and counterstained with the nuclear marker 4',6'-diamidino-2-phenylindole, dihydrochloride (DAPI). The number of DAPI cells labeled with BrdU was enumerated in five fields per coverslip under a 20× lens. At least *n* = 3 independent cultures of NSPCs grown in parallel were assessed in triplicate for each age group examined.

NSPC Differentiation

Previously established protocols were used to assess NSPC differentiation⁶. NSPCs from each age group were enzymatically dissociated and plated on poly-D-lysine and laminin-coated glass coverslips in 24 well plates. Growth factors were retrieved to induce differentiation and cells were maintained in medium consisting of Neurobasal-A with 1% GlutaMAX[™], 2% B-27, 1% Antibiotic-Antimycotic, and 2% fetal bovine serum (Atlanta Biologicals, Norcross, GA, USA). Immunocytochemical assessment of differentiation

into glial and neuronal cell types was performed after 10 days in culture. Five fields per coverslip were enumerated and the percentage of DAPI-stained cells expressing Tuj1 (neurons), glial fibrillary acidic protein (GFAP; astrocytes) or RIP (oligodendrocytes) were counted under a 20 \times lens. A total of $n = 3$ independent NSPC lines, grown in parallel, were assessed in triplicate for the analysis.

Immunocytochemistry

NSPCs plated on poly-D-lysine and laminin-coated glass coverslips were immunostained following established protocols^{6,20}. Briefly, after fixation in 4% PFA, cells were washed and blocked with 1% bovine serum albumin (BSA; Sigma-Aldrich) in 1 \times PBS (Life Technologies) containing 0.4% Triton-X-100 (Sigma-Aldrich) and 2% normal goat serum (Life Technologies). After overnight incubation at 4°C with primary antibodies, cells were treated with appropriate secondary antibodies (1:500) coupled to fluorochromes Alexa 488, 594, or 647 (Life Technologies-Molecular Probes, Grand Island, NY, USA) and counterstained with DAPI. Primary or secondary antibodies were deleted under control conditions. The concentration of the primary antibodies used were as follows: nestin (1:300, EMD Millipore, Billerica, MA, USA); neuronal class III beta-tubulin (Tuj1, 1:300; Covance, Princeton, NJ, USA); GFAP, 1:500 (EMD Millipore); RIP (1:500, EMD Millipore); Nrf2-H300 (1:200, Santa Cruz Biotechnology, Dallas, TX, USA); glutamate-cysteine ligase modifier subunit (GCLM; 1:200, Santa Cruz Biotechnology); and BrdU (1:100, Abcam, Cambridge, MA, USA).

RNA Interference and Transfection Assays

Previously established methods were used for Nrf2 knockdown or overexpression in newborn (P0) or middle-aged (15 mo) NSPCs respectively⁶. For the knockdown studies, the cells were treated with short interfering (si)RNAs (Santa Cruz Biotechnology) targeting Nrf2, control siRNAs, or PBS using Lipofectamine[®] RNAiMAX Transfection Reagent (Life Technologies). After 48 h, the medium containing the siRNA was removed, the cells washed, and replenished with new growth medium. The cells were then assessed via live-dead or BrdU assays described above. For the overexpression studies, a rat Nrf2 expression plasmid (CMV promoter, Creative Biogene Technology, Shirley, NY, USA) was transfected into NSPCs using Lipofectamine[®] LTX Reagent (Life Technologies). Parallel NSPC cultures treated with only Lipofectamine[®] LTX Reagent served as controls. After 72 h, the transfection medium was removed, cells were rinsed, and fresh growth medium was added. The transfected and control NSPCs were then analyzed via live-dead and BrdU assays.

Western Blotting

For the assessment of Nrf2 expression via western blotting, cells were harvested in radioimmunoprecipitation assay

(RIPA) buffer (Sigma-Aldrich) and sonicated before clarification at 15,000 \times g for 30 min. Cell lysates were resolved by sodium dodecyl sulfate (SDS)-polyacrylamide gel electrophoresis (PAGE) and immunoprecipitated proteins were analyzed by immunoblot with antibodies against Nrf2 H-300 (1:500, Santa Cruz Biotechnology) and beta-actin (1:500, Santa Cruz Biotechnology) diluted in blocking solution (0.1 M tris-buffered saline (TBS) with 0.1% Tween-20, and 5% dry milk) overnight at 4°C. Primary antibodies were detected with a 1 h incubation at room temperature with appropriate horseradish peroxidase (HRP)-conjugated secondaries (1:3000, Santa Cruz Biotechnology). The relative intensity of the bands was visualized using SuperSignal West Femto Max Sensitivity Substrate (ThermoFisher Scientific, Waltham, MA, USA) on an Azure c600 imaging system (Azure Biosystems, Dublin, CA, USA).

Immunohistochemistry

Immunohistochemistry was performed according to previously published protocols^{6,20}. Tissue sections were washed in 1 \times TBS (pH 7.4) solution, subjected to antigen retrieval if needed, and treated with blocking solution (10% normal goat serum, 0.5% Triton-X-100 in TBS). They were then incubated overnight at room temperature in an appropriate concentration of primary antibodies. The next day, the cells were rinsed and subjected to a 2-h incubation at room temperature with secondary antibodies (1:200) coupled to fluorochromes Alexa 488, 594, 647 (Life Technologies-Molecular Probes), or alternatively biotinylated secondary antibodies. In conditions where biotinylated secondaries were used, a tertiary streptavidin tag (Alexa 488, 555, 647; Life Technologies-Molecular Probes) was applied. All sections were finally counterstained with DAPI. Control conditions constituted the deletion of the primary antibody or secondary antibody and the inclusion of relevant isotype specific antibodies and sera instead of the omitted antibodies. Primary antibody concentrations utilized were as follows: Nrf2 (1:100, Santa Cruz Biotechnology); anti-tubulin beta 3 (TUBB3; 1:1000, Biolegend, San Diego, CA, USA); GFAP clone-GA5: (1:500, EMD Millipore); SRY (sex determining region Y)-box 2 (Sox2; 1:400, Abcam); doublecortin (Dcx; 1:1000, Abcam); minichromosome maintenance complex component 2 (MCM2; 1:200, BD Biosciences, San Jose, CA, USA); nestin (1:10, Developmental Studies Hybridoma Bank, Iowa City, IA, USA); green fluorescent protein (GFP; 1:350, Abcam); BrdU (1:100, Abcam).

EdU Staining. EdU incorporation was visualized using a Click-iT Plus reaction (ThermoFisher Scientific) according to the manufacturer's instructions with some modifications. Briefly, tissues were washed in 3% BSA-PBS, permeabilized in 0.5% Triton-X-100 in PBS, and the Click-iT cocktail (containing kit specified amounts of buffer, copper protectant, Alexa Fluor picolyl azide-647) added. After incubation at room temperature for 40 min, the cocktail was removed, and

tissue washed in 3% BSA-PBS before continuing with standard immunohistochemistry.

Stereology and Cell Counts

Stereology. Stereological probes were applied using a Zeiss Imager M2 microscope (Carl Zeiss, Jena, Germany) equipped with StereoInvestigator software (MBF Bioscience, VT, USA) according to previously published method^{6,21,22}. BrdU⁺ cells were counted using the optical fractionator under a 63× oil immersion objective in sections 420 μm apart. For all analyses, after section thickness was determined, guard zones were set (4 μm) at the top and bottom of the section that were not included in the counting area. All contours were drawn around the region of interest at 2.5× magnification. Cells were counted using a grid size of 45 × 45 μm and a counting frame size of 65 × 65 μm. The counting frame was lowered at 1–2 μm interludes and each cell in focus was marked. The Gundersen method for calculating the coefficient of error was used to estimate the accuracy of the optical fractionator results. Coefficients obtained were generally less than 0.15.

Cell Counts. In vitro, the number of DAPI-labeled NSPCs expressing Nrf2 (staining covering most of the nucleus and/or cytoplasm was considered positive) and GCLM were counted in five fields per sample under a 20× lens (Zeiss Axioimager M2). In vivo, the number of DG cells expressing Nrf2, Sox2, Dcx, MCM2 in the rats, and Sox2, Dcx, and nestin/GFAP, and MCM2 in Nrf2^{-/-} and WT mice, were counted in three adjacent sections at the same level per animal, under a 63× lens of a confocal microscope (Leica SP5-II with LAS software, Leica Microsystems, Buffalo Grove, IL, USA). Counting occurred across the entire DG on each section. For determining the number of GFP⁺ cells in grafts and the fraction expressing Tuj1 (neurons), GFAP (astrocytes), RIP (oligodendrocytes), and nestin (undifferentiated) within NSPC grafts, confocal microscopy was used as previously described²⁰. Six regions containing grafted cells (two in graft center, and four in the graft periphery) were evaluated in three adjacent sections, under a 63× lens. Data were expressed as mean ± standard error of the mean of percent of GFP⁺ cells expressing either Tuj1, GFAP, nestin or RIP cells counted per section.

Microscopy. A Zeiss AxioImager A1 (Zeiss, Jena, Germany) inverted phase microscope with an AxioCam MrC camera and Axiovision software was used to qualitatively analyze the NSPCs in culture. A Zeiss M2 Imager microscope connected to an AxioCam Mrm digital camera was used for fluorescence microscopy. Additional fluorescence analysis was performed using a Leica SP5-II confocal microscope (Leica Microsystems). Z sectioning was performed at 1–2 μm intervals in order to verify the co-localization of markers. Image extraction and analysis was conducted via the Leica LAS software.

Statistical Analyses. Sigmaplot 11 and Graphpad prism 7 software were used for statistical analyses. For comparing two groups, *t* tests were used. For comparisons between three or more groups, one-way analysis of variance (ANOVA) followed by Tukey's or Bonferroni's post-hoc test for multiple comparisons between treatment groups was conducted. Two-way repeated measures ANOVA was used to analyze the Morris water maze and pattern separation data in the aging rats across time. Differences were accepted as significant at *p* < 0.05. Additional statistical details as pertaining to each experiment are provided within the relevant results and legend sections.

Results

DG NSPCs show a Distinct Temporal Pattern of Regenerative Decline Highlighting a Critical Middle-Age Period

DG NSPCs isolated from five age-groups of rats, namely newborn (N, postnatal day 0), 2 mo (YA), 9 mo (A), 15 mo (MA), and 24 mo (O), were analyzed in vitro (Fig. 1A, B; representative images of newborn and middle-aged NSPC cultures are displayed in Fig. 1A, B). Specifically, NSPC survival (live-dead assay, Fig. 1C), proliferation (BrdU, Fig. 1D) and differentiation (immunohistochemistry, Fig. 1E–H, I) were examined. The live-dead assay indicated that the NSPC survival rate decreased until adulthood after which it remained stable until old age (*p* < 0.01, N versus A). The BrdU assay on the other hand showed a progressive decline in NSPC proliferation with age with a notable reduction noted at the MA stage (15 months, *p* < 0.001 A versus MA). In terms of differentiation, although NSPCs (nestin⁺, Fig. 1E) of all age-groups showed the ability to differentiate into neurons (Tuj1⁺, Fig. 1F), astrocytes (GFAP⁺, Fig. 1G) and oligodendrocytes (RIP⁺, Fig. 1H), a significant alteration in neuronal and glial production was noted at MA (Fig. 1I). Specifically, it was observed that while the number of Tuj1⁺ neurons significantly declined (Fig. 1I, *p* < 0.05, A versus MA), the number of GFAP⁺ astrocytes increased (Fig. 1I, *p* < 0.01, A versus MA) in the MA group. No significant changes were observed in terms of oligodendroglial differentiation (Fig 1I).

The five age-groups of animals were also subjected to a Morris water maze task (Fig. 1J) to measure hippocampal spatial learning and memory function which is known to be correlated with neurogenesis levels³⁰. Additionally, we also assessed the pattern separation ability of the animals, an important function of the DG which involves the differential encoding of closely-related memories which is more specifically connected to adult neurogenesis (Fig. 1L)³¹. Results from these behavioral tasks indicated that middle-aged and old animals had significant deficits in spatial learning and pattern separation abilities compared with the younger age-groups (Fig. 1K, M). In the water maze test, compared with young adult and adult animals, the middle-aged and old rats

required longer paths to find the hidden platform (higher CIPL scores, Fig. 1K). Similarly, in the pattern separation task, the older rats spent about the same time exploring the object in the novel context compared with the time spent exploring the object in the familiar context, suggesting that they are unable to form appropriate representation of these distinct object–context pairs (Fig. 1M). The expectation is that animals with robust levels of adult hippocampal neurogenesis will spend more time with the object in the novel context than the object in the familiar context, demarking fine discriminatory abilities. On the other hand, animals with low or absent DG neurogenesis would spend an equal amount of time with both objects, indicating inability to register subtle contextual differences. Once more it was found that the 15 mo old animals were the first group to exhibit significantly worse abilities ($p < 0.05$, MA compared with Y) in discriminating novel from familiar objects in object–context pairs.

Furthermore, to more precisely demarcate the observed critical middle-age period of NSPC vulnerability between 9 and 15 mo of age, we examined cells from two more ages of rats at 11 and 13 months. Live-dead and BrdU analysis on these age-groups indicated that there was no change in NSPC survival from 9–15 mo (Fig. S1A); however, a significant drop in proliferation (Fig. S1B) occurred during the 13 and 15 months period. There was also a significant decline in spatial cognitive ability in the water maze between 13 and 15 mo (Fig. S1C). These data suggest a specific time-period of increased vulnerability, at 13–15 months, when there is a notable reduction in DG NSPC proliferation (but not DG NSPC viability), and related behavioral function during aging.

The Decline in Nrf2 Expression Correlates with the Pattern of Decline in NSPC Regeneration with Age

Given the in vitro results, we next examined NSPC proliferation and neurogenesis in the DG across the five age-groups of rats in vivo, and studied its relationship to the NSPC's expression of the redox transcription factor, Nrf2. As depicted in Fig. 2A–F, the number of cells expressing the proliferation marker MCM2 decreased progressively, with a significant loss noted during adulthood first noted at middle age. In addition, a significant decrement in proliferation was observed from the newborn to the young adult stage. A similar pattern of decline in Sox2⁺ cells (intermediate progenitors, Fig 2.H, L, P, T, X and UU) and Dcx⁺ cells (newborn neurons, Fig 2.BB, FF, JJ, NN, RR and WW) was also determined in the DG. These data support the in vitro data (Fig. 1) indicating that adult DG NSPC proliferation and regeneration significantly deteriorates at middle age.

Corresponding to these data, we found that Nrf2 expression declined in similar manner in the DG NSPCs. As shown, the fraction of Sox2⁺ and Dcx⁺ cells co-expressing Nrf2, gradually decreased as age increased (Fig 2G–Z, AA–TT). Once more, a significant reduction in these cell populations

was seen at middle age (Fig. 2VV, XX) with a prior loss noted at the young adult stage. When NSPC Nrf2 expression was examined in vitro it was seen that, akin to NSPCs in vivo, the cells displayed a comparable pattern of reduction in Nrf2 expression (Fig. 2A–E) with a significant decrement in the number of Nrf2 expressing adult NSPCs noted at middle age (Fig. 2F). Nrf2 localization also changed with age, with a strong nuclear and cytoplasmic expression noted in the younger NSPC age-groups, with mostly small nuclear foci noted in the MA and O cells. Moreover, a similar pattern of reduction in the expression of the classical Nrf2 target gene, GCLM, was noted in the NSPCs indicating that Nrf2 activity decreased across these age-groups (Fig. 2G–L).

Nrf2 Expression Controls DG NSPC Regenerative Function in Vitro

Next, we specifically assessed the impact of Nrf2 expression on aging DG NSPC function through in vitro knockdown and overexpression assays (Fig. 3). First, newborn NSPCs were treated with siRNAs to knockdown Nrf2 expression, and its effects on NSPC survival and proliferation was then studied. It was observed that compared with controls Nrf2 knockdown significantly impaired DG NSPC survival (Fig. 3A, $p < 0.05$, siControl versus siNrf2) as well as proliferative capacity (Fig. 3B, $p < 0.001$, siControl versus siNrf2). Second, middle-aged NSPCs were transfected with Nrf2 to upregulate Nrf2 expression. Under these conditions, interestingly the survival of the cells (Fig. 3C) was not significantly affected however, the proliferation substantially improved (Fig. 3D, $p < 0.001$, untreated versus Nrf2 transfected). We additionally also assessed DG NSPCs from newborn (postnatal day 0) Nrf2 knockout (Nrf2^{-/-}) and WT (Nrf2^{+/+}) mice. It was noted that cellular survival was reduced, although not significantly, in the Nrf2^{-/-} NSPCs (Fig. 3E). However, the proliferative rate of these cells was found to be significantly lower than that of WT NSPCs (Fig. 3F). Moreover, the differentiation potential of the Nrf2^{-/-} NSPCs was also different in that these cells produced significantly lower number of Tuj1⁺ neurons ($p < 0.05$), but a higher number of GFAP⁺ astrocytes ($p < 0.05$), compared with the WT cells (Fig. 3G). Altogether, these data indicated that Nrf2 exerts a key influence on DG NSPC proliferation and differentiation, but may not be crucial for survival, in the context of aging.

Nrf2 Expression Controls DG NSPC Regenerative Function in Vivo

DG NSPCs were also studied in vivo in the Nrf2^{-/-} and WT mice through immunohistochemistry. It is known that the SGZ starts forming around postnatal day 7 and is clearly delineated only from postnatal day 14 onwards³². Hence, in newborn (P0) animals, the expression of NSPC antigens has a unique configuration different from the adult brain³². The P0 DG also lacks the primary GFAP/nestin double-positive type B NSPC population (which gives rise to the

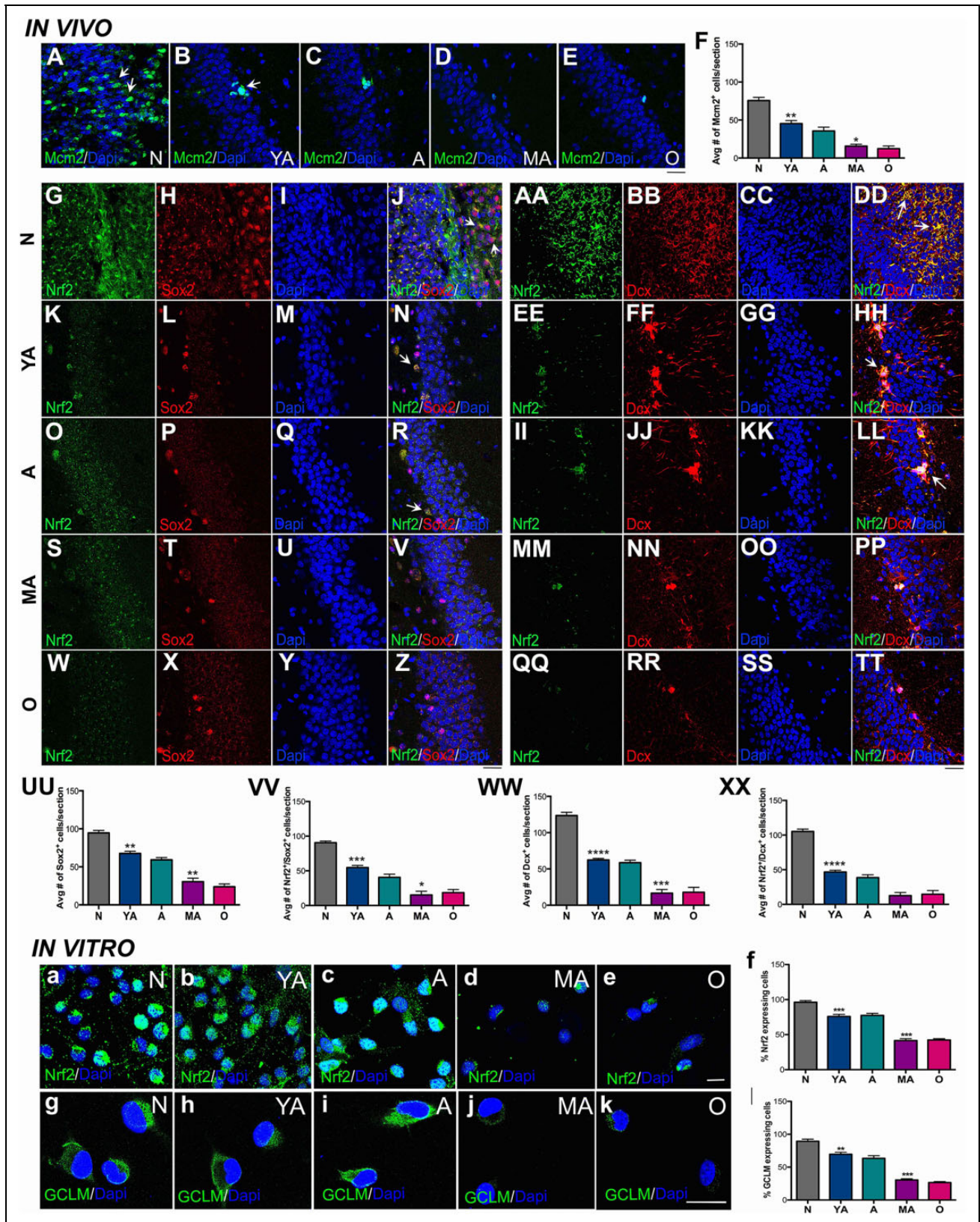


Fig. 2. Correlation of decline in DG NSPC regeneration to Nrf2 expression. Immunohistochemical analysis by age group (N, YA, A, MA and O) illustrating MCM2 staining (for proliferation) in A–E and its quantification is in F ($p < 0.01$, N versus YA and $p < 0.05$, A versus MA; one-way ANOVA with Tukey's post-hoc test). Qualitative assessment of hippocampal Sox2⁺ NSPCs and their expression of Nrf2 across the five age-groups is in G–Z, with quantification in UU ($p < 0.01$, N versus YA and $p < 0.01$, A versus MA; one-way ANOVA with Tukey's post-hoc

type C (Sox2) and type A (Dcx) cells in the adult system), and additionally expresses Dcx in a more diffuse but widespread manner compared with the adult system. It was observed that Mcm2 (Fig. 4A), Sox2 (Fig. 4C), GFAP (Fig. 4E) and Dcx (Fig. 4G) were expressed in a fashion typical for this age in WT mice³². However, expression of each of these antigens was muted in the Nrf2^{-/-} mice, suggesting a compromised NSPC proliferation and regeneration in the mice at this developmental stage (Fig. 4B, D, F, H). Interestingly, no notable changes with respect to GFAP (glial cell) expression were observed.

Adult (2.5 mo old) Nrf2^{-/-} and WT animals were also examined to understand the effects of Nrf2 loss in the aging context. Here, a significant reduction in MCM2 (Fig. 4I–K), Sox2 (Fig. 4L–N), and GFAP/nestin (Fig. 4O–Q) expressing NSPCs was noted in the DG of the Nrf2^{-/-} mice. Moreover, the number of Dcx⁺ newborn neurons was also significantly reduced in the Nrf2^{-/-} mice compared with WT controls (Fig. 4R–T). Moreover, when the animals were behaviorally tested via the Morris water maze and pattern separation tasks, the Nrf2^{-/-} animals showed significant deficits. In the water maze task, the mice showed a significantly higher CIPL score on day 1 ($p < 0.05$; Fig. 4U), suggesting slower initial learning, compared with their WT littermates. On all other days, these animals did not exhibit any significant differences, suggesting that general spatial learning is not much impaired in Nrf2^{-/-} animals. Nonetheless, in the probe trial (conducted at the end of day 4) we found that WT animals crossed the exact goal (platform) position significantly more times, than the Nrf2^{-/-} animals (Fig. 4V, $p < 0.05$)²⁶. This indicated that the Nrf2^{-/-} animals might have more subtle deficits in precise learning abilities^{14,33}.

Additionally, because previous studies have reported that animals with suppressed adult hippocampal neurogenesis show impairments in relearning a new goal position after platform reversal in the Morris water maze (Fig. S2A), we asked whether the Nrf2^{-/-} mice might show similar deficits^{33,34}. It was found that upon goal reversal, Nrf2^{-/-} animals had a higher CIPL score on day 5 (Fig. S2A), and displayed a significantly higher exploration time to find the location of the reversal platform compared with WT animals ($p < 0.05$; Fig. S2B).

Finally, in the pattern separation test, the Nrf2^{-/-} animals exhibited a compromised behavior as indicated by their substantially reduced exploration of the object in the novel context ($p < 0.05$, Fig. 4W) when compared with their WT counterparts.

All in all, these behavioral and immunohistochemical data from the transgenic mice supported an important role for Nrf2 in age-related DG NSPC regeneration and related behaviors.

Nrf2 Overexpression Improves Survival and Integration of NSPCs Transplanted into the Aging DG

Given our findings that Nrf2 expression is important for robust DG NSPC function, we next asked whether enriching the hippocampus with NSPCs overexpressing Nrf2 can improve DG neurogenesis and associated behavioral function. Our previous work has found newborn SVZ NSPCs to be capable of surviving, and inducing plasticity as well as functional effects in the brains of young adult animals^{20,21}. Therefore, we specifically transplanted 11 mo old Fisher 344 rats with newborn SVZ NSPCs overexpressing Nrf2 (experimental schematic in Fig. 5A). As a comparison, we also transplanted middle-aged NSPCs overexpressing Nrf2. Newborn or middle-aged NSPCs cells expressing only eGFP, or just buffer (sham), were administered to control animals. The cells were implanted bilaterally into both hemispheres at two sites along the rostrocaudal extent of the DG (a red star indicates the targeted location in the context of the right DG in the upper panels in Fig. 5B, and corresponding images of grafted GFP⁺ NSPCs in the right DG appear below). The animals were tested behaviorally at 15 mo of age and subsequently sacrificed to assess the histological consequences of NSPC grafting. This particular experimental timeline was chosen so as to allow for an analysis of grafted NSPC effects in relation to the previously described 13–15 mo critical period.

Nrf2 overexpression was induced via AAV2/1 viral vectors tagged with eGFP reporter, encoding Nrf2. As depicted in Fig. 5E–F, AAV2/1 robustly infected the NSPCs in vitro, and resulted in an increased expression of Nrf2 in both newborn and middle-aged NSPCs (Fig. 5B and D, western blot data in Fig. S3A) compared with controls (Fig. 5A and C, western blot data in Fig. S3A). Upon transplantation into the hippocampus, these newborn and middle-aged NSPCs were found to maintain their expression of high Nrf2 (Fig. 5G–J). It was also observed that the NSPC grafts overexpressing Nrf2 were larger, more mature, and well integrated into host tissues (contained cells with robustly developed processes extending into the host neuropil and several cells noted to be migrating from the graft) compared with controls (Fig. 5G–J, Fig. S3B: high magnification image of the periphery of a newborn Nrf2 graft). This was particularly

Fig. 2. (Continued). test), and VV ($p < 0.001$, N versus YA and $p < 0.05$, A versus MA; one-way ANOVA with Tukey's post-hoc test) are shown. Similarly, qualitative and quantitative analysis of Dcx⁺ cells is in AA–TT, WW ($p < 0.0001$, N versus YA and $p < 0.001$, A versus MA; one-way ANOVA with Tukey's post-hoc test) and XX ($p < 0.0001$, N versus YA and $p < 0.01$, A versus MA; one-way ANOVA with Tukey's post-hoc test). Expression of Nrf2 and GCLM in cultured hippocampal NSPCs across the five age-groups is shown in a–e and g–k, with quantification in f ($p < 0.001$, N versus YA and $p < 0.001$, A versus MA; one-way ANOVA with Tukey's post-hoc test) and l ($p < 0.01$, N versus YA and $p < 0.001$, A versus MA; one-way ANOVA with Tukey's post-hoc test). * $p < 0.05$, ** $p < 0.01$, *** $p < 0.001$. Scale bars: A–E; G–Z, AA–TT: 25 μ m, a–e: 15 μ m. A: adult; ANOVA: analysis of variance; DG: dentate gyrus; N: newborn; GCLM: glutamate–cysteine ligase modifier subunit; MA: middle-aged; NSPC: neural stem progenitor cell; O: old; YA: young adult.

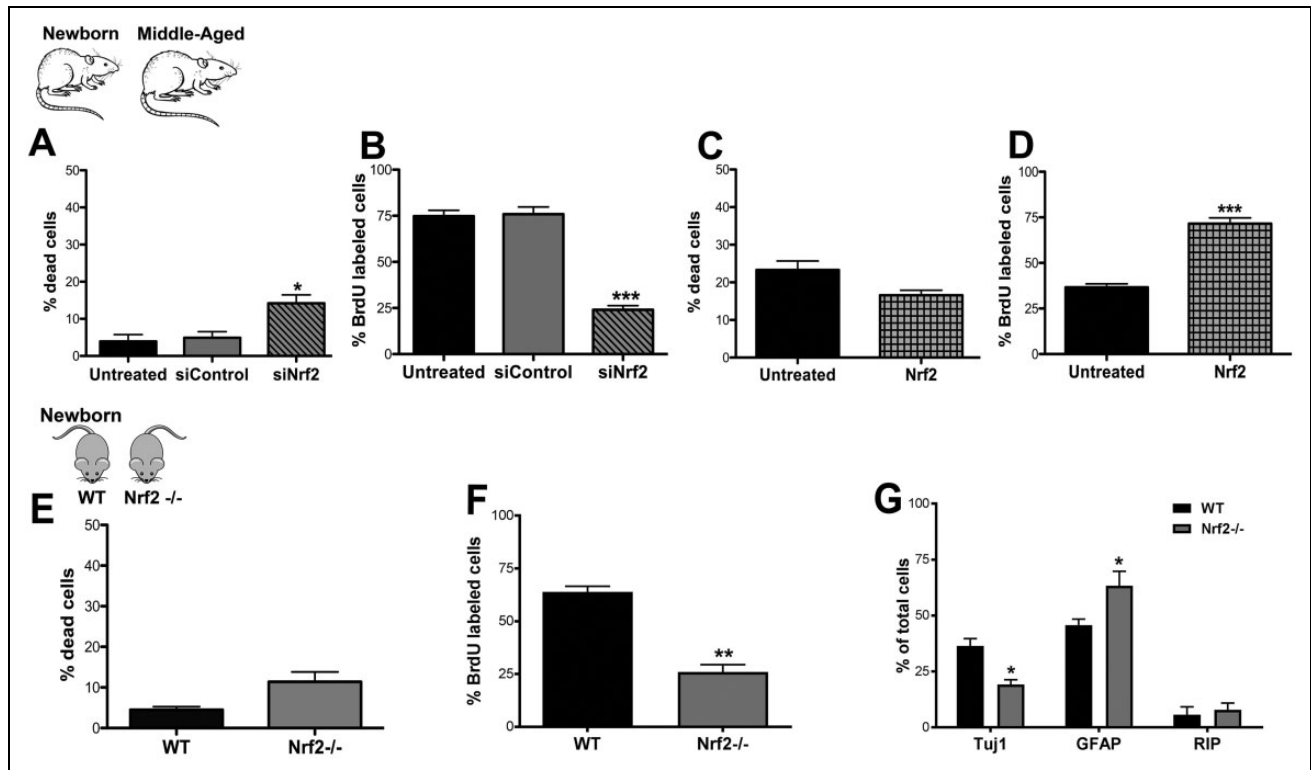


Fig. 3. Effects of altered Nrf2 expression on DG NSPC regeneration in vitro. Graphs A and B show results from live-dead (viability) and BrdU (proliferation) assays performed on untreated, control siRNA, and Nrf2 siRNA-treated (siNrf2) newborn rat hippocampal NSPCs ($p < 0.05$, $p < 0.001$, U/siC versus siNrf2, unpaired t tests). Panels C and D show the viability and proliferation of untreated middle-aged cells compared with those transfected with Nrf2 ($p < 0.001$, U versus Nrf2). The in vitro survival and proliferative function of DG NSPCs isolated from Nrf2^{-/-} mice compared with WT mice is depicted in E and F ($p < 0.01$, unpaired t tests). The capacity of newborn Nrf2 WT and Nrf2^{-/-} NSPCs to differentiate into TuJ1⁺ neurons ($p < 0.05$, unpaired t test), GFAP⁺ astrocytes ($p < 0.05$, unpaired t test), and RIP⁺ oligodendrocytes is in (G). * $p < 0.05$, ** $p < 0.01$, *** $p < 0.001$. BrdU: bromodeoxyridine; DG: dentate gyrus; GFAP: glial fibrillary acidic protein; NSPC: neural stem progenitor cell.

evident in animals receiving newborn NSPC grafts (Fig. 5H versus 5G). The middle-aged grafts were quite small compared with the newborn grafts; however, larger implants were noted in the animals receiving the Nrf2 overexpressing middle-aged cells (Fig. 5J versus 5I). The quantification of GFP⁺-transplanted cells confirmed these impressions, and determined that there were significantly ($p < 0.05$) greater numbers of surviving cells in newborn grafts overexpressing Nrf2 compared with grafts expressing eGFP-only (Fig. 5K). Moreover, the number of cells in Nrf2 overexpressing middle-aged grafts was also higher (although not significantly, $p > 0.05$) compared with control middle-aged grafts transduced with just eGFP (Fig. 5K).

The animals were also behaviorally assessed via the pattern separation task. Here it was found that at 11 mo of age, that is at baseline and before transplantation, all rats explored the object in the novel patterned context more than the familiar context (Fig. 5L, N). This pattern separation potential was lost in non-grafted control animals after 4 mo, at 15 mo of age, as expected (Fig. 5M, O). However, it was found to be significantly ($p < 0.05$, novel versus

familiar) better in animals grafted with newborn Nrf2 overexpressing NSPCs (Fig. 5M). In fact, the average exploration time of the novel object, increased from 58.5% at 11 mo, to 68.2% at 15 mo of age, in the rAAV-Nrf2-eGFP animals. Interestingly, it was also found that the animals implanted with newborn rAAV-eGFP NSPCs maintain the efficiency with which they differentiate novel from familiar at 11 and 15 mo, compared with control non-grafted animals which lose this ability from 11 to 15 mo. On the other hand, animals grafted with middle-aged NSPCs with high Nrf2 showed no significant improvement in the pattern separation task (Fig. 5O). Overall, these data correspond well with the graft viability data (Fig. 5K), and indicate that newborn grafts overexpressing Nrf2 survive better to induce functionally meaningful effects in the aging DG.

Nrf2 Overexpressing Grafts show Improved Neurogenesis and Enhance Host Regeneration

NSPC grafts were immunohistochemically probed to determine their differentiation and proliferation potential.

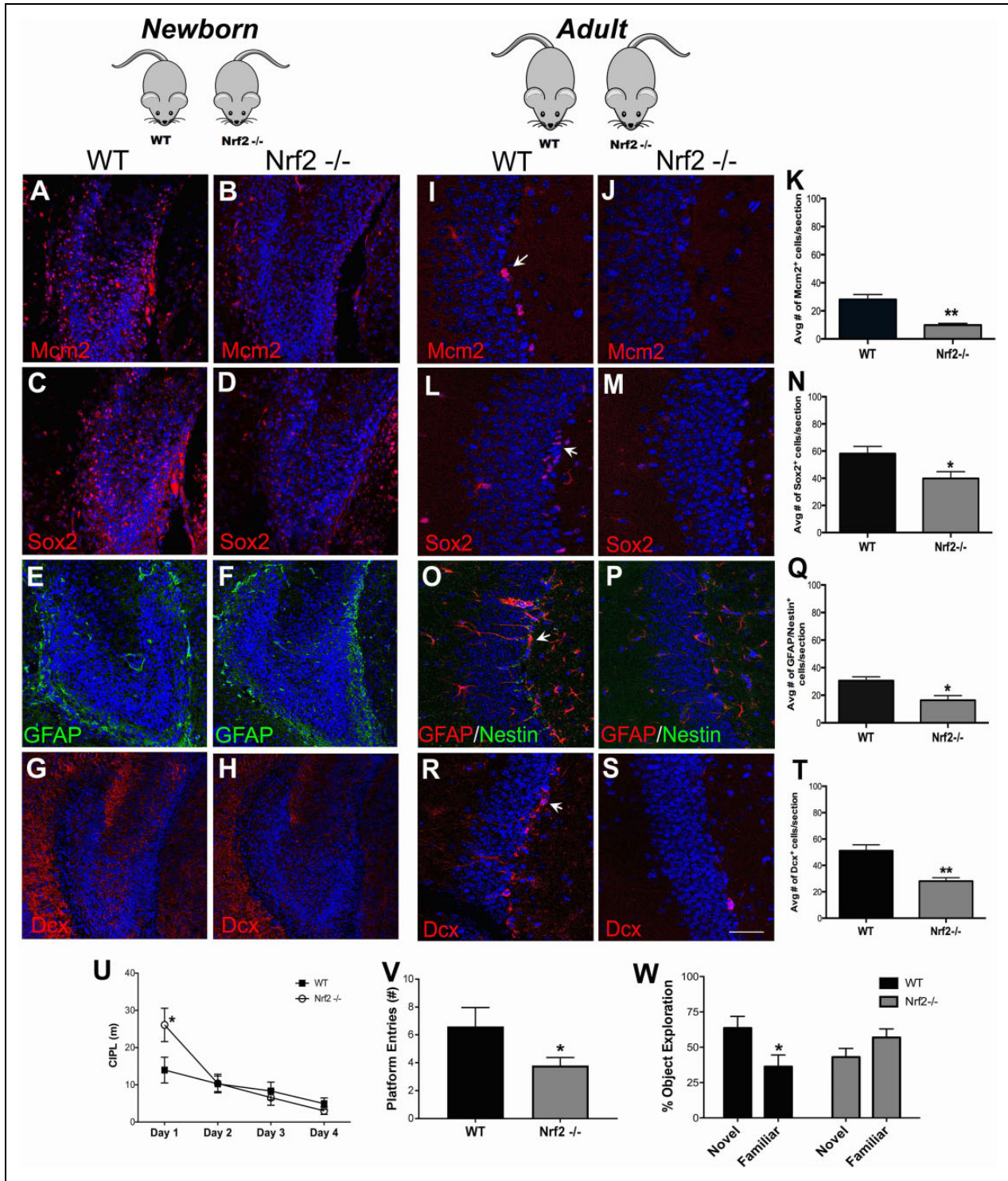


Fig. 4. In vivo assessment of DG NSPCs from Nrf2 knockout mice. In vivo immunohistochemical analysis of the DG NSPCs in newborn Nrf2 WT and Nrf2^{-/-} mice using antibodies targeting MCM2 (proliferation; A–B), Sox2 (proliferating neural progenitors; C–D), GFAP (astrocytes; E–F) and Dcx (neuroblasts; G–H) was performed. NSPCs from adult Nrf2 WT and knockout animals were also assessed: MCM2 (I–K), Sox2 (L–N), GFAP/nestin (O–Q) and Dcx (R–T). Behavioral analysis of young adult Nrf2 WT and knockout mice through the Morris water maze task is shown in U, and the number of platform entries in the probe trial is in V ($p < 0.05$, unpaired t tests). Behavioral results from the pattern separation task is in W ($p < 0.05$, unpaired t tests). * $p < 0.05$, ** $p < 0.01$. Scale bars: A–H: 60 μ m, I–S: 30 μ m. DG: dentate gyrus; GFAP: glial fibrillary acidic protein; NSPC: neural stem progenitor cell.

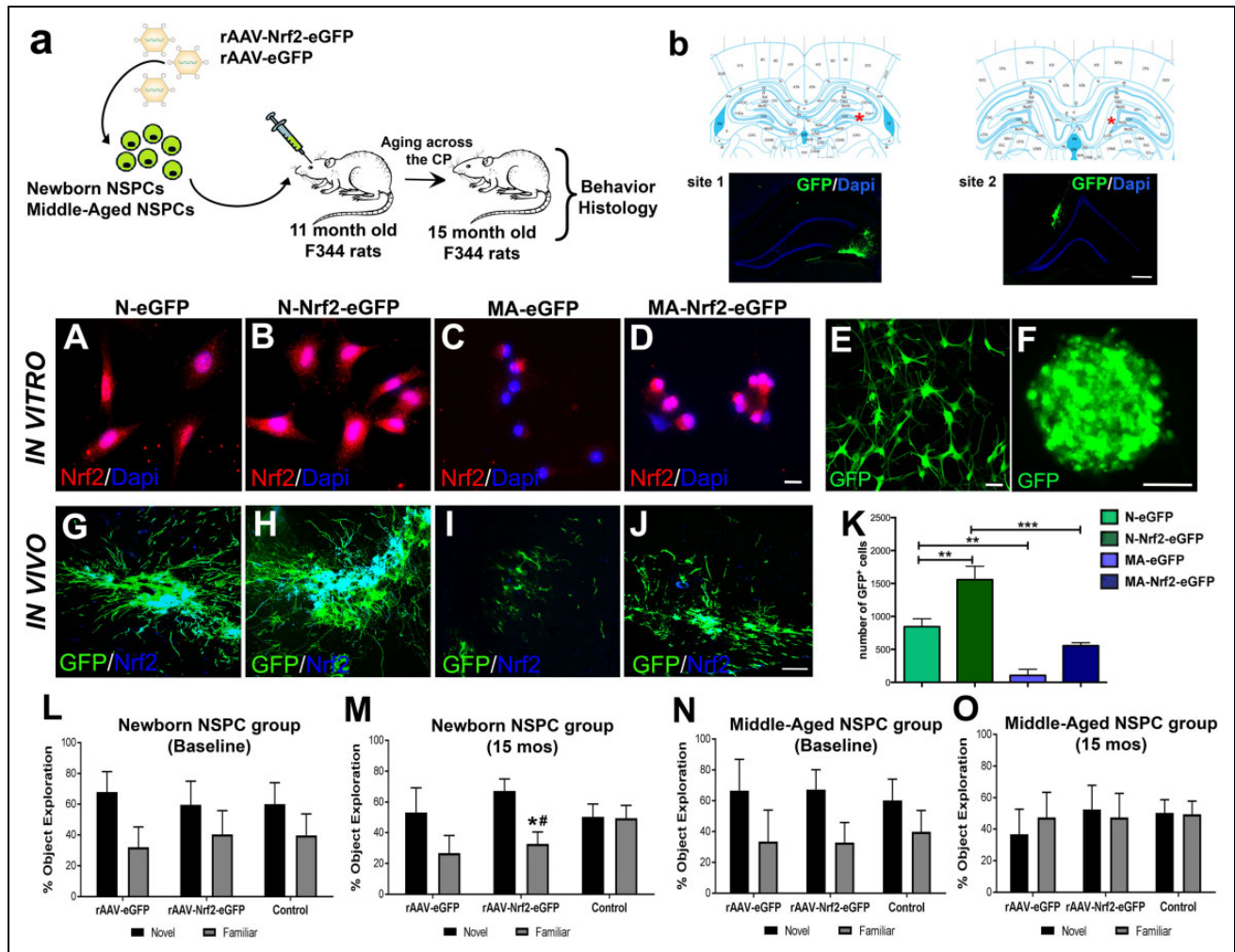


Fig. 5. Characterization of NSPC transplants overexpressing Nrf2 and their behavioral effects across the critical period. (A) Schematic of the experimental design illustrating that newborn and middle-aged NSPCs were transduced with an eGFP tagged AAV2/1 virus with or without Nrf2. These cells were transplanted into the DG of 11-month-old rats and the animals aged through the CP of NSPC decline. Behavioral and histological analysis was performed at age 15 months of age. Stereotaxic transplantation sites are noted in B with corresponding fluorescence confirmation of GFP⁺ graft locations. Nrf2 expression in newborn (N) and middle-aged (MA) NSPCs with or without viral Nrf2 transduction is in A–D. Representation of AAV2/1 transduced NSPC cultures, as single-cell and neurospheres, before grafting is in E and F. In vivo Nrf2 expression of GFP⁺ transplants are in G–J (newborn grafts (G–H) and middle-aged grafts (I–J)). Quantification of grafted cells in the different experimental groups is in K ($p < 0.01$ N-eGFP versus N-Nrf2-eGFP; $p < 0.01$, N-eGFP versus MA-eGFP; $p < 0.001$, N-Nrf2-eGFP versus MA-Nrf2-eGFP; one-way ANOVA with post-hoc Tukey's test). Results from the pattern separation task, conducted on naïve 11-month-old animals before transplantation (baseline) are in L, N, and after the CP at 15 mo are in M, O ($*p < 0.05$, novel versus familiar in animals implanted with newborn grafts overexpressing Nrf2, $\#p < 0.05$ compared with control). $*p < 0.05$, $**p < 0.01$, $\#p < 0.05$. Scale bars: B: 200 μ m, A, C–D: 20 μ m, E: 25 μ m, F: 100 μ m, G–J: 50 μ m. ANOVA: analysis of variance; CP: critical period; DAPI: 4',6'-diamidino-2-phenylindole, dihydrochloride; DG: dentate gyrus; GFP: green fluorescent protein; NSPC: neural stem progenitor cell; eGFP: enhanced green fluorescent protein.

Specifically, the percentage of GFP⁺ grafted cells expressing nestin (undifferentiated, Fig. 6A–C), Tuj1 (neurons, Fig. 6E–G), GFAP (astrocytes, Fig. 6I–K), and RIP (oligodendrocytes, Fig. 6M–O) was quantified to assess differentiation. Also, the percentage of GFP⁺ cells labeled with EdU was quantified to examine proliferation (Fig. 6Q–S). EdU had been administered to the animals 2 mo after transplantation in order to label any proliferating cells in the graft at this time point. Results from these analyses indicated that there were no significant differences in the fraction of

undifferentiated nestin⁺ cells present in newborn grafts overexpressing Nrf2, compared with control eGFP-only grafts (Fig. 6D). On the other hand, newborn grafts overexpressing Nrf2 showed significantly increased neuronal differentiation ($p < 0.05$, Fig. 6H), reduced astroglial differentiation ($p < 0.05$, Fig. 6L), and no notable differences in terms of oligodendroglial production (Fig. 6P), compared with control grafts. In contrast, the middle-aged grafts contained lower percentages of nestin⁺, Tuj1⁺ and RIP⁺ cells, but higher GFAP⁺ astrocytes, compared with

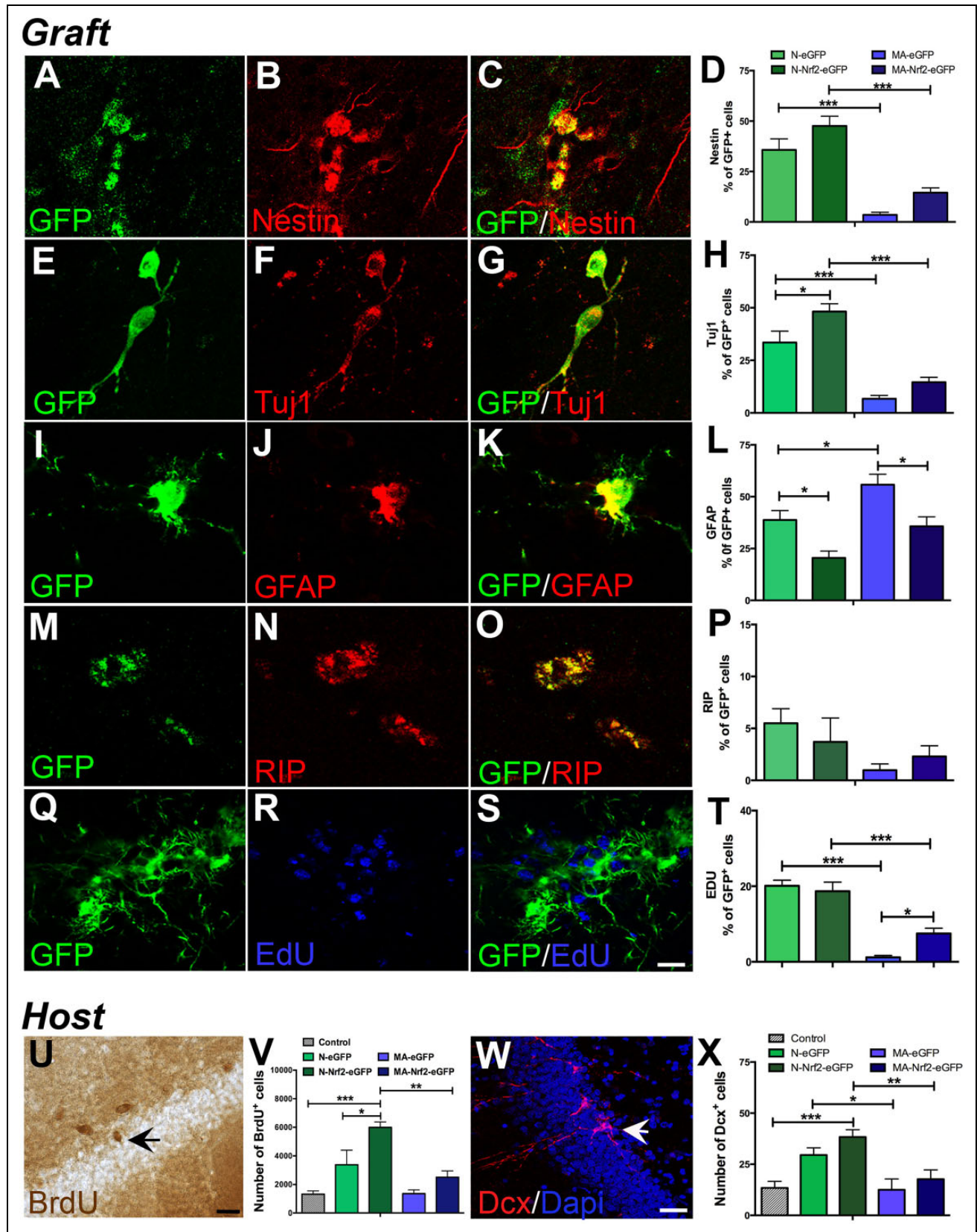


Fig. 6. Quantification of grafted NSPC phenotype and the induction of host DG plasticity. Examples of grafted (GFP⁺) undifferentiated NSPCs (nestin⁺, A–C) and their differentiation into Tuj1⁺ neurons (E–G), GFAP⁺ astrocytes (I–L), and RIP⁺ oligodendrocytes (M–O). The quantifications of nestin, Tuj1, GFAP and RIP expressing cells within the newborn and middle-aged grafts are in D, H, L, P. Graft proliferation, assessed via the quantification of EdU incorporation, is in Q–T. On the other hand, host DG NSPC proliferation was examined via BrdU

newborn grafts (Fig. 6D, H, L, P). However, the middle-aged grafts overexpressing Nrf2 showed a significant reduction in the percentage of astrocytes compared with eGFP-only controls, similar to the case with the newborn grafts (Fig. 6L). With regards to graft proliferation, middle-aged grafts overexpressing Nrf2 showed a significant increase in the percentage of EdU⁺ cells, whereas no differences were found in the newborn grafts (Fig. 6T). Moreover, we also found an integration of grafted cells into the DG in four of the seven animals transplanted with newborn NSPCs overexpressing Nrf2, but not in any of the other groups (Fig. S3C, D). Such integration was mostly noted at the lateral edge of the upper blade of the DG (Fig. S3C), and sometimes more centrally in the upper DG (Fig. S3D). Overall, these data illustrate that augmentation of Nrf2 expression altered the fate of the grafted cells, supporting neurogenesis and inhibiting astrogliogenesis, and possibly promoted the integration of NSPCs into host tissues.

We additionally assessed the effects of NSPC grafting on host DG NSPC proliferation and neurogenesis. Animals had been administered BrdU before the transplantation, to allow for the examination of host neurogenesis independently from grafted cells (which were only EdU/GFP⁺). Unbiased stereological analysis indicated that there were greater numbers of BrdU⁺ cells (Fig. 6U) in the DG of animals grafted with both newborn NSCs overexpressing Nrf2, as well control newborn NSPCs (with only eGFP), compared with non-grafted controls (Fig. 6V). However, no significant increases in BrdU labeled cells were noted in animals receiving middle-aged grafts (Fig. 6V). When endogenous neurogenesis was specifically assessed via the quantification of Dcx⁺ cells (Fig. 6W), it was determined that animals that had received implants of Nrf2 overexpressing and control newborn NSPCs, had higher number of Dcx⁺ cells in the host DG compared with controls (Fig. 6X). However, animals administered middle-aged grafts showed no differences with regards to Dcx cell numbers (Fig. 6X). These data indicated that both host proliferation and neurogenesis had been enhanced by the grafting of particularly the newborn Nrf2 overexpressing cells.

Discussion

This study for the first time demonstrates the importance of the Nrf2 transcription factor in age-related DG NSPC function. Specifically, our results indicate that a diminishing Nrf2 expression compromises the regenerative ability of DG NSPCs, resulting in a specific temporal pattern of decline in hippocampal neurogenesis during aging, which

is cognitively relevant. The results also indicate that enriching the aged DG environment with NSPCs overexpressing Nrf2 can mitigate this neurogenic decline and improve cognitive abilities.

Firstly, our data delineate a particular critical middle-age period of vulnerability in DG NSPC regenerative function during aging. Utilizing seven groups of rats spanning the aging spectrum (0, 2, 9, 11, 13, 15 and 24 mo of age) we found that the proliferative capacity of cultured DG NSPCs decreases significantly during a defined 13–15 mo time-period during adulthood. The differentiation profile of the NSPCs was also significantly altered at middle age (15 mo) in that neuronal production declined but astroglial production increased notably. On the other hand, the survival of DG NSPCs remained relatively stable from young-adulthood until old age (24 mo). Importantly, these fundamental NSPC changes in vitro mirrored the temporal pattern of NSPC changes in vivo which translated into observable deficits in neurogenesis-related behaviors, namely spatial learning in the Morris water maze and pattern separation in an object–context recognition task. Overall, these data align with other studies in the literature that report a decrement in DG neurogenesis by middle age, but also more precisely demarcate and characterize the middle-age time-period at cellular and behavioral levels^{35–37}. Interestingly, in contrast with aging SVZ NSPCs (the focus of our previous work), which exhibit a strong decline in survival during the critical period, DG NSPC survival does not appear to be affected⁶. These results emphasize reduced proliferation and reduced neurogenic capacity as the prominent features of DG NSPC aging, and concur with recent studies which suggest a transition to a quiescent state, rather than a frank loss of stem cells, as underlying the drop in DG regeneration with age³⁸.

Secondly, our data implicate Nrf2 expression as vital to maintaining DG NSPC regeneration in the aging context. In rats, a reduction in Nrf2 expression was found to correlate closely with the decline of NSPC proliferation and neurogenesis with age. Additionally, the knockdown of Nrf2 in young NSPCs significantly decreased NSPC proliferation, whereas Nrf2 overexpression in old NSPCs increased proliferation. Furthermore, NSPCs from Nrf2 knockout mice showed muted regenerative abilities both in vitro and in vivo, and the knockout mice exhibited behavioral impairments in the water maze and pattern separation tasks. Here, as with the rat data, the effects of Nrf2 loss were more pronounced on DG NSPC proliferation and neuronal differentiation, than on cell survival. However, Nrf2 knockdown (via siRNAs) in the rat cells significantly affected cell viability, indicating that Nrf2's effects on DG NSPC survival

Fig. 6. (Continued). labeling (example in U). Stereological quantification of host BrdU⁺ cells in various NSPC transplanted groups is shown in the graph in V. Dcx⁺ neuroblasts (example in W) were enumerated in the host DG (in X). **p* < 0.05, ***p* < 0.01, ****p* < 0.001, one-way ANOVA with post-hoc Tukey's tests. Scale bars: A: 20 μm; U, W: 30 μm. ANOVA: analysis of variance; BrdU: bromodeoxyuridine; Dcx: doublecortin; DG: dentate gyrus; EdU: 5-ethynyl-2'-deoxyuridine; GFAP: glial fibrillary acidic protein; GFP: green fluorescent protein; NSPC: neural stem progenitor cell.

cannot be completely discounted. Nevertheless, these data overall suggest that reduced Nrf2 may potentially be involved in the NSPC's shift to quiescence. The results corroborate a recent study by Robledinos-Antón et al., that investigated Nrf2's control of DG NSPC function in Nrf2 knockout animals¹⁹. The novelty of the present results lies in the more detailed cellular and behavioral analysis of Nrf2's impact on DG NSPC function, as well as in exploring Nrf2's effects from the normal aging perspective. In essence, these data convey for the first time that Nrf2 acts as a major governor of age-related DG NSPC behavior and fate, influencing specific neurogenesis-related cognitive functions.

With regards to cognitive aspects, our studies show that Nrf2 knockout animals display impairments in the initial acquisition of a spatial location in the Morris water maze task, as well as learning a reversal of this location and in the pattern separation task, both of which are more directly connected to DG NSPC function^{27,30,31,33}. The finding that Nrf2 knockout mice did not show major deficits, except on day 1, in the Morris water maze suggests that general spatial learning remains mostly intact in these animals. Nevertheless, the significantly reduced number of goal crossings during the probe trial by the Nrf2 knockout animals, compared with their WT littermates, indicates that while the knockout animals are able to develop an allocentric cognitive map that allows for escape during the learning phase, these maps may not be sufficiently precise. Studies by Garthe et al., 2014 also show that probe trial performance, but not broad spatial learning, are impaired in cyclin D2 knockout mice with constitutively suppressed adult hippocampal neurogenesis³³. Additionally, animals with deficits in hippocampal neurogenesis have been previously shown to have impairments in reversal learning sometimes interpreted as reflecting a deficit in cognitive flexibility resulting from reduced neurogenesis^{30,33,39}. Thus, our finding that Nrf2 knockout animals require longer exploration times to find the reversal platform compared with their WT littermates suggest that reduced Nrf2 plays a role in neurogenesis-related cognitive flexibility. Lastly, in terms of the object–context recognition task that probed pattern separation, our results indicate that the Nrf2 knockout animals are significantly impaired on this critical function known to be dependent on the DG. Moreover, these data are supported by other studies which report that animals with impaired DG neurogenesis display deficits in tasks that require the encoding of closely-related memories^{18,31,40–42}. Thus, in the end, the behavioral results indicate that Nrf2 knockout mice are not generally impaired in terms of spatial learning in the water maze, suggesting that Nrf2 may not play a robust part in mediating broad hippocampal networks or functions. However, deficits in the reversal aspect of the water maze and pattern separation behavior, which are more neurogenesis-specific, delineate a highly specific role of Nrf2 in the DG NSPCs and in facilitating DG neurogenesis.

Thirdly, our data show that the transplantation of high Nrf2 expressing NSPCs into the aged hippocampus, can

counteract the decline in DG proliferation and neurogenesis-related to the critical middle-age period. We found that newborn NSPCs overexpressing Nrf2, implanted into 11-month-old animals, were able to improve host DG proliferation and neurogenesis across time, resulting in higher levels of both at 15 mo of age. Critically, this effect was associated with a significant improvement in the pattern separation abilities of these animals. Nevertheless, we also remark that these behavioral data would be strengthened and would allow for better interpretation from the inclusion of more animals. Moreover, the viability, integration, and neurogenic differentiation of the newborn grafts overexpressing Nrf2 was substantially better than that of control newborn grafts without Nrf2. These data indicate that Nrf2 overexpression improves the survival and function of grafted newborn NSPCs and alleviates host DG NSPC vulnerability during the critical period. Our previous studies have shown that newborn NSPCs can survive and induce plasticity in the brain of young adult animals upon transplantation^{20,21,43}. It was also shown in these studies that specific trophic factors secreted by the implanted NSPCs were responsible for the effects seen, which may also be a possibility in the current studies. However, it is also known that the survival and function of the NSPCs is compromised upon implantation into the brain of old animals⁴⁴. A recent report has shown that NSPCs from postnatal day 2 old rats treated with the brain-derived neurotrophic factor (BDNF) before implantation can survive and differentiate well in both the young and old hippocampus⁴⁵. In this context, our current results demonstrate that increased Nrf2 can significantly promote transplanted newborn NSPC survival, differentiation and integration upon, in relation to a critical period of age-related DG vulnerability, and lead to improvement in host neurogenesis and meaningful behavioral effects. Moreover, our data with the middle-aged grafts also indicate that although the age of the donor cells at the time of transplantation is important, increased Nrf2 may be capable of supporting the survival and neurogenic function of 'older' cells.

In conclusion, our study specifies a role for Nrf2 expression in determining hippocampal neural stem cell aging. It also indicates that DG NSPC function can be rescued via the transplantation of young Nrf2-overexpressing NSPCs. Nrf2's ability to activate a range of antioxidant and other cellular stress-resistance genes, and in maintaining intracellular redox balance, a known central regulator of NSPC function, probably drives these effects^{46–50}. In fact, it has been shown that redox deficits caused by an upstream reduction in Nrf2 levels arise in hippocampal tissues during aging⁵¹. This implies a broad and powerful redox-based regulatory influence of Nrf2 on DG regenerative function, the understanding of which has significant implications for both fundamental NSPC biology as well as the development of therapeutics, via targeting activation of the Nrf2 pathway, for age-related cognitive disorders.

Acknowledgements

We are truly grateful to Dr Beverly Davidson (Childrens Hospital of Philadelphia, CHOP, PA, USA) for her advice on the construction and use of the viral vectors. We also acknowledge Xueyuan Liu (Director) and members of the CHOP Viral Vector Core for generating the AAV vectors. We additionally extend our thanks to Doug Cromey and Patty Jansma for the technical assistance with confocal microscopy.

Author Contributions

L. Madhavan – Conception and design, collection and assembly of data, data analysis and interpretation, manuscript writing, financial support, and final approval of the manuscript.

S. Ray and M. J. Corenblum – Conception and design, collection and assembly of data, data analysis and interpretation, and manuscript writing.

A. Anandhan – Collection and assembly of data, data analysis, and manuscript editing.

A. Reed and F. O. Ortiz – Collection of data, and manuscript editing.

D. D. Zhang – Provision of study material, experimental design, and manuscript editing.

C. A. Barnes – Experimental design, provision of experimental resources, and manuscript editing.

L. Madhavan, S. Ray, and M. J. Corenblum contributed equally to the performance of experimental work.

Ethical Approval

Ethical approval to report this case was obtained from The University of Arizona Institutional Animal Care and Use Committee, Tucson, AZ, USA.

Statement of Human and Animal Rights

All animal procedures in this study were conducted in accordance with regulations of NIH and Institutional Guidelines on the Care and Use of Animals, and The University of Arizona Institutional Animal Care and Use Committee approved all experimental procedures.

Statement of Informed Consent

There are no human subjects in this article and informed consent is not applicable.

Declaration of Conflicting Interests

The authors declared no potential conflicts of interest with respect to the research, authorship, and/or publication of this article.

Funding

The authors disclosed receipt of the following financial support for the research, authorship, and/or publication of this article: This work was supported by intramural funds from the University of Arizona and an Arizona Biomedical Research Commission (ADHS14-082982) grant to L. Madhavan, and the McKnight Brain Research Foundation.

Supplemental Material

Supplementary material for this article is available online.

References

- Alvarez-Buylla A, Lim DA. For the long run: maintaining germinal niches in the adult brain. *Neuron*. 2004;41(5):683–686.
- Doetsch F. A niche for adult neural stem cells. *Curr Opin Genet Dev*. 2003;13(5):543–550.
- Conover JC, Shook BA. Aging of the subventricular zone neural stem cell niche. *Aging Dis*. 2011;2(1):49–63.
- Encinas JM, Michurina TV, Peunova N, Park JH, Tordo J, Peterson DA, Fishell G, Koulakov A, Enikolopov G. Division-coupled astrocytic differentiation and age-related depletion of neural stem cells in the adult hippocampus. *Cell Stem Cell*. 2011;8(5):566–579.
- Liu L, Rando TA. Manifestations and mechanisms of stem cell aging. *J Cell Biol*. 2011;193(2):257–266.
- Corenblum MJ, Ray S, Remley QW, Long M, Harder B, Zhang DD, Barnes CA, Madhavan L. Reduced Nrf2 expression mediates the decline in neural stem cell function during a critical middle-age period. *Aging Cell*. 2016.
- Lee JM, Li J, Johnson DA, Stein TD, Kraft AD, Calkins MJ, Jakel RJ, Johnson JA. Nrf2, a multi-organ protector? *FASEB J*. 2005;19(9):1061–1066.
- Bryan HK, Olayanju A, Goldring CE, Park BK. The Nrf2 cell defence pathway: Keap1-dependent and -independent mechanisms of regulation. *Biochem Pharmacol*. 2013;85(6):705–717.
- Zhang DD, Hannink M. Distinct cysteine residues in Keap1 are required for Keap1-dependent ubiquitination of Nrf2 and for stabilization of Nrf2 by chemopreventive agents and oxidative stress. *Mol Cell Biol*. 2003;23(22):8137–8151.
- Suzuki T, Yamamoto M. Stress-sensing mechanisms and the physiological roles of the Keap1-Nrf2 system during cellular stress. *J Biol Chem*. 2017;292(41):16817–16824.
- Baird L, Dinkova-Kostova AT. The cytoprotective role of the Keap1-Nrf2 pathway. *Arch Toxicol*. 2011;85(4):241–272.
- Hochmuth CE, Biteau B, Bohmann D, Jasper H. Redox regulation by Keap1 and Nrf2 controls intestinal stem cell proliferation in *Drosophila*. *Cell Stem Cell*. 2011;8(2):188–199.
- Holmstrom KM, Baird L, Zhang Y, Hargreaves I, Chalasani A, Land JM, Stanyer L, Yamamoto M, Dinkova-Kostova AT, Abramov AY. Nrf2 impacts cellular bioenergetics by controlling substrate availability for mitochondrial respiration. *Biol Open*. 2013;2(8):761–770.
- Wakabayashi N, Chartoumpakis DV, Kensler TW. Crosstalk between Nrf2 and Notch signaling. *Free Radic Biol Med*. 2015.
- Zhu J, Wang H, Sun Q, Ji X, Zhu L, Cong Z, Zhou Y, Liu H, Zhou M. Nrf2 is required to maintain the self-renewal of glioma stem cells. *BMC Cancer*. 2013;13:380.
- Malhotra D, Portales-Casamar E, Singh A, Srivastava S, Arenillas D, Happel C, Shyr C, Wakabayashi N, Kensler TW, Wasserman WW and others. Global mapping of binding sites for Nrf2 identifies novel targets in cell survival response through ChIP-Seq profiling and network analysis. *Nucleic Acids Res*. 2010;38(17):5718–5734.
- Apple DM, Solano-Fonseca R, Kokovay E. Neurogenesis in the aging brain. *Biochem Pharmacol*. 2017;141:77–85.

18. Goncalves JT, Schafer ST, Gage FH. Adult Neurogenesis in the Hippocampus: From Stem Cells to Behavior. *Cell*. 2016; 167(4):897–914.
19. Robledinos-Antón N, Rojo AI, Ferreira E, Nunez A, Krause KH, Jaquet V, Cuadrado A. Transcription factor NRF2 controls the fate of neural stem cells in the subgranular zone of the hippocampus. *Redox Biol*. 2017;13:393–401.
20. Madhavan L, Daley BF, Davidson BL, Boudreau RL, Lipton JW, Cole-Strauss A, Steece-Collier K, Collier TJ. Sonic Hedgehog Controls the Phenotypic Fate and Therapeutic Efficacy of Grafted Neural Precursor Cells in a Model of Nigrostriatal Neurodegeneration. *PLoS One*. 2015;10(9):e0137136.
21. Madhavan L, Daley BF, Sortwell CE, Collier TJ. Endogenous neural precursors influence grafted neural stem cells and contribute to neuroprotection in the parkinsonian rat. *Eur J Neurosci*. 2012;35(6):883–895.
22. Corenblum MJ, Flores AJ, Badowski M, Harris DT, Madhavan L. Systemic human CD34(+) cells populate the brain and activate host mechanisms to counteract nigrostriatal degeneration. *Regen Med*. 2015;10(5):563–577.
23. Zeng C, Pan F, Jones LA, Lim MM, Griffin EA, Sheline YI, Mintun MA, Holtzman DM, Mach RH. Evaluation of 5-ethynyl-2'-deoxyuridine staining as a sensitive and reliable method for studying cell proliferation in the adult nervous system. *Brain Res*. 2010;1319:21–32.
24. Barnes CA, Suster MS, Shen J, McNaughton BL. Multistability of cognitive maps in the hippocampus of old rats. *Nature*. 1997; 388(6639):272–275.
25. Vorhees CV, Williams MT. Morris water maze: procedures for assessing spatial and related forms of learning and memory. *Nat Protoc*. 2006;1(2):848–858.
26. Gallagher M, Burwell R, Burchinal M. Severity of spatial learning impairment in aging: development of a learning index for performance in the Morris water maze. *Behav Neurosci*. 1993;107(4):618–626.
27. Franca TFA, Bitencourt AM, Maximilla NR, Barros DM, Monserrat JM. Hippocampal neurogenesis and pattern separation: A meta-analysis of behavioral data. *Hippocampus*. 2017;27(9): 937–950.
28. Dere E, Huston JP, De Souza Silva MA. The pharmacology, neuroanatomy and neurogenetics of one-trial object recognition in rodents. *Neurosci Biobehav Rev*. 2007;31(5):673–704.
29. Jain S, Yoon SY, Zhu L, Brodbeck J, Dai J, Walker D, Huang Y. Arf4 determines dentate gyrus-mediated pattern separation by regulating dendritic spine development. *PLoS One*. 2012; 7(9):e46340.
30. Garthe A, Kempermann G. An old test for new neurons: refining the Morris water maze to study the functional relevance of adult hippocampal neurogenesis. *Front Neurosci*. 2013;7:63.
31. Johnston ST, Shtrahman M, Parylak S, Goncalves JT, Gage FH. Paradox of pattern separation and adult neurogenesis: A dual role for new neurons balancing memory resolution and robustness. *Neurobiol Learn Mem*. 2016;129:60–68.
32. Nicola Z, Fabel K, Kempermann G. Development of the adult neurogenic niche in the hippocampus of mice. *Front Neuroanat*. 2015;9:53.
33. Garthe A, Huang Z, Kaczmarek L, Filipkowski RK, Kempermann G. Not all water mazes are created equal: cyclin D2 knockout mice with constitutively suppressed adult hippocampal neurogenesis do show specific spatial learning deficits. *Genes Brain Behav*. 2014;13(4):357–364.
34. Zhang CL, Zou Y, He W, Gage FH, Evans RM. A role for adult TLX-positive neural stem cells in learning and behaviour. *Nature*. 2008;451(7181):1004–1007.
35. Rao MS, Hattiangady B, Shetty AK. The window and mechanisms of major age-related decline in the production of new neurons within the dentate gyrus of the hippocampus. *Aging Cell*. 2006;5(6):545–558.
36. Hattiangady B, Rao MS, Shetty GA, Shetty AK. Brain-derived neurotrophic factor, phosphorylated cyclic AMP response element binding protein and neuropeptide Y decline as early as middle age in the dentate gyrus and CA1 and CA3 subfields of the hippocampus. *Exp Neurol*. 2005;195(2):353–371.
37. Marlatt MW, Potter MC, Lucassen PJ, van Praag H. Running throughout middle age improves memory function, hippocampal neurogenesis, and BDNF levels in female C57BL/6 J mice. *Dev Neurobiol*. 2012;72(6):943–952.
38. Lugert S, Basak O, Knuckles P, Haussler U, Fabel K, Gotz M, Haas CA, Kempermann G, Taylor V, Giachino C. Quiescent and active hippocampal neural stem cells with distinct morphologies respond selectively to physiological and pathological stimuli and aging. *Cell Stem Cell*. 2010;6(5):445–456.
39. Anacker C, Hen R. Adult hippocampal neurogenesis and cognitive flexibility - linking memory and mood. *Nat Rev Neurosci*. 2017;18(6):335–346.
40. Sahay A, Scobie KN, Hill AS, O'Carroll CM, Kheirbek MA, Burghardt NS, Fenton AA, Dranovsky A, Hen R. Increasing adult hippocampal neurogenesis is sufficient to improve pattern separation. *Nature*. 2011;472(7344):466–470.
41. Yassa MA, Stark CE. Pattern separation in the hippocampus. *Trends Neurosci*. 2011;34(10):515–525.
42. Oomen CA, Bekinschtein P, Kent BA, Saksida LM, Bussey TJ. Adult hippocampal neurogenesis and its role in cognition. *Wiley Interdiscip Rev Cogn Sci*. 2014;5(5):573–587.
43. Madhavan L, Daley BF, Paumier KL, Collier TJ. Transplantation of subventricular zone neural precursors induces an endogenous precursor cell response in a rat model of Parkinson's disease. *J Comp Neurol*. 2009;515(1):102–115.
44. Limke TL, Rao MS. Neural stem cell therapy in the aging brain: pitfalls and possibilities. *J Hematother Stem Cell Res*. 2003;12(6):615–623.
45. Shetty AK, Hattiangady B. Grafted subventricular zone neural stem cells display robust engraftment and similar differentiation properties and form new neurogenic niches in the young and aged hippocampus. *Stem Cells Transl Med*. 2016;5(9): 1204–1215.
46. Ivanova NB, Dimos JT, Schaniel C, Hackney JA, Moore KA, Lemischka IR. A stem cell molecular signature. *Science*. 2002; 298(5593):601–604.
47. Madhavan L, Ourednik V, Ourednik J. Increased “vigilance” of antioxidant mechanisms in neural stem cells potentiates their

- capability to resist oxidative stress. *Stem Cells*. 2006;24(9): 2110–2119.
48. Madhavan L, Ourednik V, Ourednik J. Neural stem/progenitor cells initiate the formation of cellular networks that provide neuroprotection by growth factor-modulated antioxidant expression. *Stem Cells*. 2007.
49. Ramalho-Santos M, Yoon S, Matsuzaki Y, Mulligan RC, Melton DA. “Stemness”: transcriptional profiling of embryonic and adult stem cells. *Science*. 2002;298(5593):597–600.
50. Madhavan L. Redox-based regulation of neural stem cell function and Nrf2. *Biochem Soc Trans*. 2015;43(4): 627–631.
51. Ghosh D, LeVault KR, Brewer GJ. Dual-energy precursor and nuclear erythroid-related factor 2 activator treatment additively improve redox glutathione levels and neuron survival in aging and Alzheimer mouse neurons upstream of reactive oxygen species. *Neurobiol Aging*. 2014;35(1): 179–190.